Case Report

J Korean Soc Radiol 2020;81(1):190-196
https://doi.org/10.3348/jksr.2020.81.1.190
pISSN 1738-2637 / eISSN 2288-2928

대한영상의학회지

Focal Xanthogranulomatous Pyelonephritis Associated with Xanthogranulomatous Cholecystitis: A Case Report

황색육아종성 담낭염과 병발된 국소성 황색육아종성 신우신염: 증례 보고

Soong Moon Cho, MD[1], Ho Kyun Kim, MD[1]*, Hye Kyung Lee, MD[2], Byungmo Lee, MD[3], Ki Hwan Kim, MD[1], Kyoung Eun Lee, MD[1], Jae-Chan Shim, MD[1], Dae Hyun Hwang, MD[1], Ghi Jai Lee, MD[1]

Departments of [1]Radiology, [2]Pathology, [3]General Surgery, Seoul Paik Hospital, Inje University College of Medicine, Seoul, Korea

Xanthogranulomatous inflammation is a rare inflammatory reaction, characterized by lipid-laden macrophages, known as xanthomas, in histopathologic examination. Aggressive xanthogranulomatous inflammation often manifests as local infiltration but does not affect distant organs unless combined with rare systemic diseases. We report a case of focal xanthogranulomatous pyelonephritis (XGP) associated with severe xanthogranulomatous cholecystitis. Focal XGP was suspected in radiologic examination that showed a cystic lesion with an infiltrative margin, which were surgically resected and confirmed in pathologic examination. To our knowledge, this is the first report of focal xanthogranulomatous pyelonephritis associated with xanthogranulomatous cholecystitis. Moreover, we found peripheral hypointensity around the cystic lesion in the T2-weighted image, probably reflecting hemorrhage and fibrosis of the xanthogranulomatous inflammation.

Index terms Xanthogranulomatous Cholecystitis; Pyelonephritis, Xanthogranulomatous; Magnetic Resonance Imaging

INTRODUCTION

Xanthogranulomatous inflammation (XGI) is a rare abnormal inflammatory response, found mainly in gallbladder (GB) and kidney. Biliary obstruction and abnormal response to hemorrhage are main pathophysiology of xanthogranulomatous cholecystitis (XGC). Likewise, diffuse type xanthogranulomatous pyelonephritis (XGP) mostly accompanies

Received April 25, 2019
Revised May 13, 2019
Accepted July 9, 2019

***Corresponding author**
Ho Kyun Kim, MD
Department of Radiology, Seoul Paik Hospital, Inje University College of Medicine, 9 Mareunnae-ro, Jung-gu, Seoul 04551, Korea.

Tel 82-2-2270-0139
Fax 82-2-2266-6799
E-mail kyhkim@hanmail.net

ORCID iDs
Soong Moon Cho
https://orcid.org/0000-0002-2109-2317
Ho Kyun Kim
https://orcid.org/0000-0003-0576-271X
Hye Kyung Lee
https://orcid.org/0000-0002-1648-8827
Byungmo Lee
https://orcid.org/0000-0002-6998-0727
Ki Hwan Kim
https://orcid.org/0000-0002-6911-8125
Kyoung Eun Lee
https://orcid.org/0000-0002-9667-4186
Jae-Chan Shim
https://orcid.org/0000-0001-7442-2079
Dae Hyun Hwang
https://orcid.org/0000-0003-1995-6312
Ghi Jai Lee
https://orcid.org/0000-0001-8300-5090

obstructive uropathy while less common focal type of XGP does not. Because there is no definite characteristic clinical or radiologic findings for XGI, it often requires surgery to be diagnosed. Lipid-laden macrophages or histiocytes are hallmark of XGI seen on histopathology (1). Here we present a case of synchronous involvement of XGI at GB and kidney focusing on radiologic findings.

CASE REPORT

A 56-year-old male patient visited gastroenterology outpatient department for ongoing weight loss, anorexia, and abdominal discomfort for 3 months. He had no past medical history and no recent medication history. He complained mild abdominal discomfort on right upper quadrant worsening when he lay down on back. He had lost his body weight from 75 kg to 55 kg during last 3 months. Vital sign and general physical examination was unremarkable. Initial laboratory tests revealed normocytic normochromic anemia as decreased hemoglobin count of 9.3 g/dL (normal range: 13–17 g/dL) and also made suggestion of biliary disease as increased alkaline phosphatase (ALP) of 133 U/L (normal range: 40–129 U/L). On the initial urine analysis, pyuria of 10–19/HPF white blood cell (normal range: 0–4/HPF) and bacteriuria of 30/HPF (normal value: 0) were detected.

Abdominal ultrasonogram revealed a 2.9 cm nodular stone in the lumen of GB with diffuse mass-like mural thickening. Intramural low- or anechoic portions were also identified (Fig. 1A). On abdominal CT, GB showed diffuse wall thickening with a few intramural nodular low-attenuations (Fig. 1A). Pericholecystic hyperemic change was noted along GB bed of hepatic parenchyma. XGC was considered and the possibility of tumorous condition such as adenocarcinoma was also considered. MRI of upper abdomen demonstrated an oval GB stone and diffuse wall thickening as heterogeneous intermediate signal intensity (SI) on T1-weighted images (T1WI) with intramural irregular cystic change (Fig. 1B). At right renal cortex, a focal soft tissue density with fuzzy margin was found in CT with intralesional non-enhancing low attenuated portion (Fig. 1C). Renal cortical abscess, hemorrhagic or infected cyst as well as tumorous lesion was considered. This lesion on MRI showed a cystic lesion with low SI rim on T2WI (Fig. 1D). For pathologic diagnosis as well as removal of GB and renal lesions, the patient was referred to hepatobiliary surgery department and underwent cholecystectomy and partial right nephrectomy. During operation, contracted GB with severe adhesion to transverse colon, duodenum, and omentum was found. GB wall was diffusely irregularly thickened. After confirming that it was not GB cancer, XGC and XGP by intraoperative frozen section biopsy, entire GB with local adhesive lesion to the transverse colon and the lateral cortex of the mid to upper portion of the right kidney with adhesive perirenal tissue were resected.

In pathologic examination, all specimens revealed chronic active XGI, with absence of any pyogenic abscess, tuberculosis, carcinoma or other neoplasm. The GB is disfigured with prominent irregular mural fibrous thickening, multifocal extensive mucosal ulcers, transmural old hemorrhages and multiple yellowish xanthogranulomatous nodules or plaques (Fig. 1E), with a large cholesterol stone. Microscopically, yellowish nodules are composed of nodular aggregates of foamy histiocytes, containing abundant lipid droplets or hemosiderin granules, admixed with severe polymorphic lympho-reticular inflammatory cells and fibroblasts were not-

ed in GB wall (Fig. 1E), transverse colonic subserosal & serosal fibroadiopose tissue and right renal cortex (Fig. 1F) and perirenal fibroadipose tissue, consistent with XGI. His final diagnosis was 1) chronic active XGC with focal mural perforation and local invasion to omentum and subserosa of transverse colon and 2) sequentially developed the focal type of chronic active XGP. He was treated with intravenous ciprofloxacin and discharged as symptoms subsided.

Fig. 1. Focal xanthogranulomatous pyelonephritis associated with xanthogranulomatous cholecystitis in a 56-year-old man, presenting with right upper quadrant pain.
A. On ultrasonography (left panel), a GB stone is seen as a curvilinear hyper-reflective echo with distal acoustic shadowing. A few anechoic nodules (arrows) are noted within the thickened isoechoic GB walls. Axial CT (right panel) shows diffuse wall thickening of GB with intramural low-attenuation nodules.
B. Axial T2- (left panel) and T1-weighted imaging (right panel) show oval GB stones as a dark signal and intramural nodules as a high signal.
C. Axial CT shows a cystic lesion in the right kidney with infiltration extending peripherally to the perirenal tissues and hepatorenal recess. Coronal CT better illustrates the infiltrative lesion between the liver and the kidney with focal peritoneal wall thickening.
GB = gallbladder

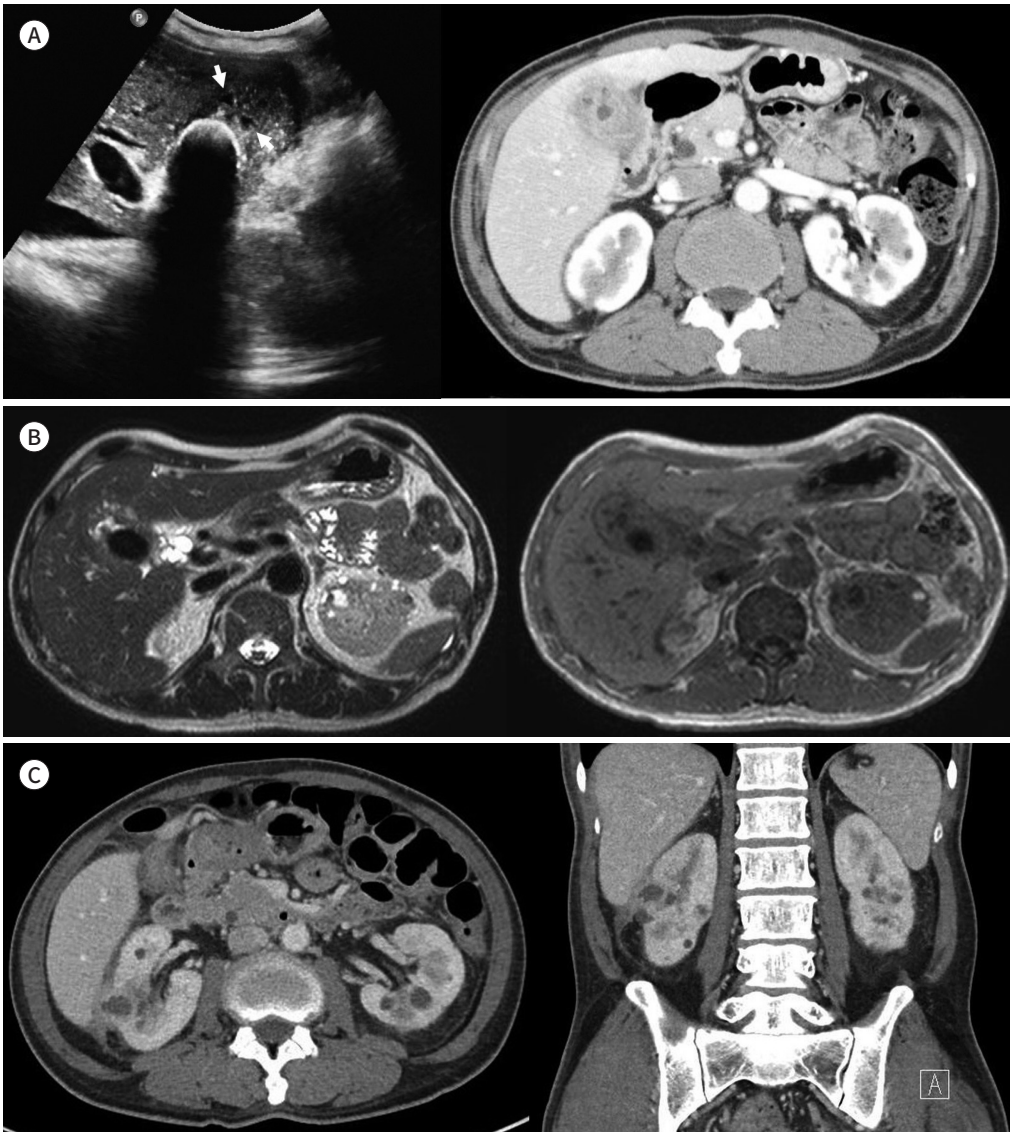

Fig. 1. Focal xanthogranulomatous pyelonephritis associated with xanthogranulomatous cholecystitis in a 56-year-old man, presenting with right upper quadrant pain.
D. Axial T2-weighted imaging (left panel) shows a nodular hyperintense lesion with rim-like low signal intensity (arrow). This lesion is not clearly outlined on the T1-weighted image (right panel).
E. The gross specimen of GB shows disfigurement with marked irregular mural fibrous thickening, multifocal extensive mucosal ulcers, transmural old hemorrhages, and multiple yellowish xanthogranulomatous nodules or plaques (left panel). Scanning photomicrograph of GB wall exhibiting mucosal ulcers, transmural hemorrhages, dense mural fibrosis, and nodular aggregates of foamy histiocytes and inflammatory cells (right panel, × 40, H&E stain).
F. The gross specimen of the right renal cortex and perirenal fibroadipose tissues (left panel) reveal a few prominent yellowish xanthogranulomatous nodules or plaques, fresh-to-old hemorrhages, and dense fibrous adhesion. Scanning photomicrography shows massive perirenal (a) and subcapsular (c) collection of foamy histiocytes, dense pericapsular fibrosis (b), and inflammatory cell infiltration (middle panel, × 40, H&E stain). Yellowish xanthogranulomatous nodules demonstrate abundant lipid-laden foamy histiocytes and hemosiderin-laden histiocytes, admixed with polymorphic lymphoreticular cells and fibroblasts (right panel, × 200, H&E stain).
GB = gallbladder, H&E = hematoxylin and eosin

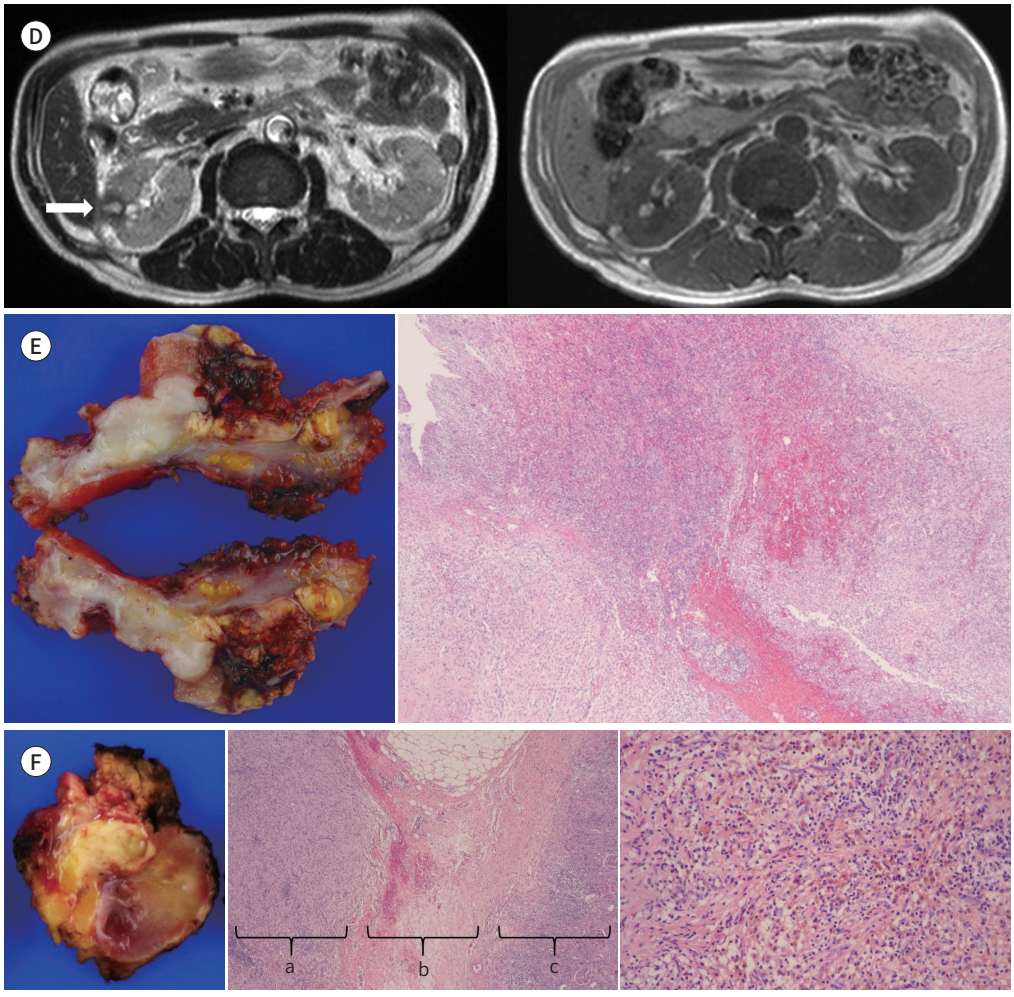

DISCUSSION

XGI, characterized by aggregation of lipid-laden foamy macrophages, usually occurs at GB and kidney but some rare histiocytoses or genetic diseases can be considered when other atyp-

ical portions of body are involved in young patients (1). Most XGCs are preceded by calculous or tumorous biliary obstruction. In the same way, most of XGP is caused by chronic urinary tract obstruction presenting as diffuse type involving entire kidney whereas only 10–15% presents as focal type without relevance to urinary obstruction. Pathophysiology of focal type XGP is still not clear (2). In the presented case, focal type XGP was incidentally founded along with typical XGC, and such case has never been reported in English literature.

In our case, focal type XGP can be explained by two mechanisms; secondary involvement from XGC or independent manifestation as systemic process. As XGI tends to involve neighboring organs, XGC has been reported to infiltrate to extrahepatic bile duct, stomach, duodenum, colon, and liver and to make fistula toward skin (1). For us, adjacent invasion of XGC was histologically confirmed in omentum and transverse colon. Also, along the inferior aspect of right hepatic lobe, infiltrative density was featured in CT, having adjacency with right side focal type XGP (Fig. 1C). Retroperitoneal extension of GB pathology could be explained when posterior pericholecystic erosion and posterior parietal peritoneum is infiltrated (3). Even in case of XGC with xanthogranulomatous pseudotumor at left side diaphragm, localized infiltration through potential anatomic route rather than remote seeding was considered (4).

In the latter hypothesis, on the other hand, focal type XGP can develop independently from XGC. Multifocal systemic XGI can be found in histiocytic process such as Erdheim-Chest disease, Rosai-Dorfman disease, hemophagocytic lymphohistiocytosis, and juvenile xanthogranuloma. Inherited lysosomal disorders also result systemic XGI. However, these diseases usually affect young age patients at different target organs like bones and vessels (1). In the presented case, such organs were clinically and radiologically intact. Moreover, related systemic pathology such as bleeding tendency and dyslipidemia were not observed in the laboratory analysis. In histopathologic examination, focal type XGP seemed to protrude inwardly from perirenal tissue toward renal cortex (Fig. 1F). Therefore, we assumed our focal type XGP as secondary invasion from primary XGC more likely than multifocal systemic involvement. This case is meaningful to propose a new pathogenesis of focal type XGP. Secondary focal type XGP was previously described only in one case so far, originating from duodenal diverticulum (5).

Our case is also valuable in that it shows unprecedented MRI findings of focal type XGP. Known MRI findings of focal type XGP include usual cystic nature of cavitary fluid with possible fluid-fluid level. Cavitary border can be seen as intermediate SI on T1 and T2WI and may enhance when introduced with intravenous gadolinium. If present, perirenal strands can be hypointense on T1 and T2WI (6). Our case showed a cavitary lesion of slightly high SI with rim-like hypointensity on T2WI. Considering chronicity of our case, rim-like T2-shortening may be related to hemorrhage and fibrosis (7). Pathologic analysis found multistage hemorrhage with hemosiderin-laden histiocytic accumulation and pericapsular organizing fibrosis (Fig. 1F). Because peripheral low SI in T2WI is a nonspecific finding, renal abscess and renal tumor with central necrosis should be on the list of radiologic differential diagnosis. On T1WI, central portion of the lesion was indistinguishable with renal parenchyma, suggesting protein-rich fluid. In contrast to T2WI, peripheral portion on T1WI was isointense, assuming that presence of xanthoma cell may compensate for T1-lengthening effect of hemosiderin and fibrosis (8).

Clinical information of the patient could make better diagnosis but had limited value in this

case. When compared with GB cancer, the most important differential diagnosis of XGC, abdominal pain, fever, and jaundice are more frequent in XGC patients. Leukocytosis, serum bilirubin, serum ALP and weight loss were invalid to differentiate between XGC and GB cancer (9). Weight loss is more frequently observed in XGP than in XGC and other usual symptoms of XGP include fever and flank pain (2). Considering size and severity, it was reasonable to regard weight loss and abdominal pain of our patient as result of XGC. Although pyuria and bacteria are also common in XGP, renal lesion of the presented case seemed too subtle for these urine abnormalities which were possibly due to superimposed acute pyelonephritis. In absence of fever and leukocytosis as in our case, radiologic finding played crucial role in making diagnosis.

In conclusion, focal type XGP can develop in association with XGC as localized infiltration. In focal type XGP, MRI may depict focal infiltrative cystic lesion with peripheral low SI rim in T2WI, resulting from hemosiderin and fibrosis.

Author Contributions

Conceptualization, K.H.K., L.B., L.H.K.; data curation, K.H.K., L.B., L.H.K., C.S.M.; investigation, C.S.M.; methodology, C.S.M., L.K.E., K.K.H.; project administration, K.H.K., L.H.K.; resources, L. H.K., L.B.; software, H.D.H., L.G.J.; supervision, K.H.K., L.H.K., L.G.J., H.D.H.; visualization, L.H.K., S.J.; writing—original draft, C.S.M.; and writing—review & editing, L.H.K., K.H.K.

Conflicts of Interest

The authors have no potential conflicts of interest to disclose.

REFERENCES

1. Bourm KS, Menias CO, Ali K, Alhalabi K, Elsayes KM. Spectrum of xanthogranulomatous processes in the abdomen and pelvis: a pictorial review of infectious, inflammatory, and proliferative responses. *AJR Am J Roentgenol* 2017;208:475-484
2. Kuo CC, Wu CF, Huang CC, Lee YJ, Lin WC, Tsai CW, et al. Xanthogranulomatous pyelonephritis: critical analysis of 30 patients. *Int Urol Nephrol* 2011;43:15-22
3. Kaushik R, Attri AK. Choleretroperitoneum-an unusual complication of cholelithiasis. *Indian J Surg* 2004; 66:358-360
4. Roels K, Bogaert J, Van Hoe L, Vanbeckevoort D, Delvaux S. Xanthogranulomatous cholecystitis associated with a xanthogranulomatous pseudotumour on the left diaphragm. *Eur Radiol* 1999;9:1139-1141
5. Losanoff JE, Reichman TW, Steinberg GD, Millis JM. Duodenal diverticulum causing xanthogranulomatous pyelonephritis with multiorgan involvement: first case report. *Digestion* 2006;74:236-237
6. Verswijvel G, Oyen R, Van Poppel H, Roskams T. Xanthogranulomatous pyelonephritis: MRI findings in the diffuse and the focal type. *Eur Radiol* 2000;10:586-589
7. Song YS, Lee IS, Choi KU, Cho KH, Lee SM, Lee YH, et al. Soft tissue masses showing low signal intensity on T2-weighted images: correlation with pathologic findings. *J Korean Soc Magn Reson Med* 2014;18:279-289
8. Cakmakci H, Tasdelen N, Obuz F, Yilmaz E, Kovanlikaya A. Pediatric focal xanthogranulomatous pyelonephritis: dynamic contrast-enhanced MRI findings. *Clin Imaging* 2002;26:183-186
9. Chang BJ, Kim SH, Park HY, Lim SW, Kim J, Lee KH, et al. Distinguishing xanthogranulomatous cholecystitis from the wall-thickening type of early-stage gallbladder cancer. *Gut Liver* 2010;4:518-523

대한영상의학회지

황색육아종성 담낭염과 병발된 국소성 황색육아종성 신우신염: 증례 보고

조숭문[1] · 김호균[1*] · 이혜경[2] · 이병모[3] · 김기환[1] · 이경은[1] · 심재찬[1] · 황대현[1] · 이기재[1]

황색육아종성 염증은 드문 염증 반응으로서 조직병리학적으로 지방을 함유한 큰포식세포의 집단인 황색종의 소견이 특징적이다. 이 질환은 공격적 성향을 보여 종종 주변으로 국소 침습하지만, 원격 장기를 침범하는 경우는 매우 드물어 전신질환이 있는 경우에 극히 예외적으로 관찰된다. 우리는 영상의학적 검사에서 주변부 침윤을 동반한 낭성 병변으로 보이는 증례에서 심한 황색육아종성 담낭염과 드물지만 국소성 황색육아종성 신우신염을 의심하였고 수술적 절제를 통해 병리학적으로 황색육아종성 담낭염에 연관되어 병발한 국소형 황색육아종성 신우신염을 확진하였다. 우리가 아는 한, 황색육아종성 담낭염에 국소성 황색육아종성 신우신염이 병발한 경우는 이전에 보고된 바가 없다. 또한, MRI T2 강조 영상에서의 낭성 병변 주위로 아마도 황색육아종성 염증의 출혈과 섬유화를 반영할 것으로 추정되는 저신호 강도 주변부를 확인하였다.

인제대학교 의과대학 서울백병원 [1]영상의학과, [2]병리과, [3]일반외과